DETERMINATION OF CLOSE APPROACHES BASED ON ELLIPSOIDAL THREAT VOLUMES

Vincent Coppola[†]

James Woodburn[+]

A method for computing close approach events for space objects having ellipsoidal threat volumes is presented. An event is deemed to occur whenever the closest distance between the an ellipsoid about a satellite of interest and an ellipsoid about another orbiting object is less than an user-specified threshold. The dimensions of each ellipsoid, representing the position uncertainty of an object, is also user-specified. Both fixed and time-varying ellipsoids are considered. We first describe the solution to the problem of computing the closest distance between a point and an ellipsoid. We then use this solution in an iterative scheme to compute the closest distance between two ellipsoids.

INTRODUCTION

In light of the increasing number of objects in orbit about the Earth and the construction of the International Space Station (ISS), the determination of close approaches between objects is becoming an increasingly important aspect of satellite operations. A study by Jenkins and Schumacher[1] indicates the growing importance of close approach prediction for the Shuttle and the Mir space station. Alfriend et al.[2] recently presented work focusing on the probability of collision of space debris with the ISS. Typical conjunction analyses determine the risk to a particular satellite of interest, the primary object, posed by the set of all other orbiting objects, the secondary objects. To be useful, analyses of conjunction events must provide a metric that may be used to determine when the risk of collision is unacceptably large.

One common measure of the risk of collision is the distance between two objects at the point of closest approach as determined from the nominal ephemeris. A simple decision rule is then constructed stating that any conjunctions with a specified minimum separation distance provide reason for concern. The separation distance is selected to be much larger than the actual physical dimensions of the bodies involved to account for uncertainty in the

[†] Senior Astrodynamics Engineer, Analytical Graphics, Inc.
[+] Chief Orbital Scientist, Analytical Graphics, Inc.

nominal ephemerides. To improve the efficiency of detecting close approaches based on minimum separation distance, Hoots et al.[3] designed a series of three filters through which secondary objects must pass before a final determination of the minimum separation distance is made. The filters serve to eliminate the majority of the objects in the catalogue and greatly reduce the number of computations needed. A special adaptation of the algorithms presented in Hoots et al.[3] has been developed to allow for efficient predictions of close approaches for entire constellations of satellites[4]. Other authors have approached restricted versions of the minimum separation distance problem considering only the distance between the orbital paths[4] or only circular orbits[5]. While the computation of close approaches based on the minimum separation distance is efficient, it assumes that the uncertainty in the position of each body is the same in all directions. This assumption leads to the detection of an excessive number of conjunctions due to the need to consider the direction of greatest uncertainty. Alfriend et al.[2] stressed the desire to minimize the number of reported close approaches for applications such as the ISS due to the high cost of performing maneuvers to avoid collisions.

The use of a minimum separation distance may also be thought of as using spherical threat volumes about the primary and secondary objects. Conjunctions occur when the threat volumes have an intersection. The sum of the radii of the threat volumes is equal to the minimum separation distance. Using this definition of a conjunction, it is possible to use shapes other than spheres to represent the threat volumes. Current Space Shuttle operations predict the entry of secondary objects into a box centered at the predicted Space Shuttle location with fixed in-track, radial and cross-track dimensions[2]. Alfano and Negron[7,8] developed an algorithm allowing for the specification of an ellipsoidal threat volume about the primary. In these cases, filtering methods may still be used to eliminate the vast majority of secondary objects from consideration and threat volumes about the secondary objects are not used. In this study, a formulation that allows for the specification of ellipsoidal threat volumes about the primary and the secondary objects is presented.

FORMULATION

The threat volumes are defined as triaxial ellipsoids centered at the predicted locations of the primary and secondary objects. The orientations of the ellipsoids relative to a common reference frame are assumed to be known. Conjunction intervals are defined as periods of time when the distance between the ellipsoid about the primary and an ellipsoid about a secondary object are smaller than a specified threshold. The crossings of this threshold are determined based on a time history of the distance between the ellipsoids. The dimensions and orientation of the ellipsoids are allowed to vary with time, but it is assumed that all dimensions of the ellipsoids are always greater than zero.

Consider two ellipsoids E and $\overline{E}$ with primary semi-axis lengths of (a,b,c) and $(\overline{a},\overline{b},\overline{c})$ respectively. The primary axes of each ellipsoid describe a natural coordinate system for each ellipsoid, also denoted by E and $\overline{E}$. Let $\vec{R} = (X,Y,Z)^T$ locate the relative distance vector between the centers of the ellipsoids, expressed in E. Let M denote the

rotation matrix that transforms between E and $\overline{E}$. The geometry of the problem is illustrated in Figure 1.
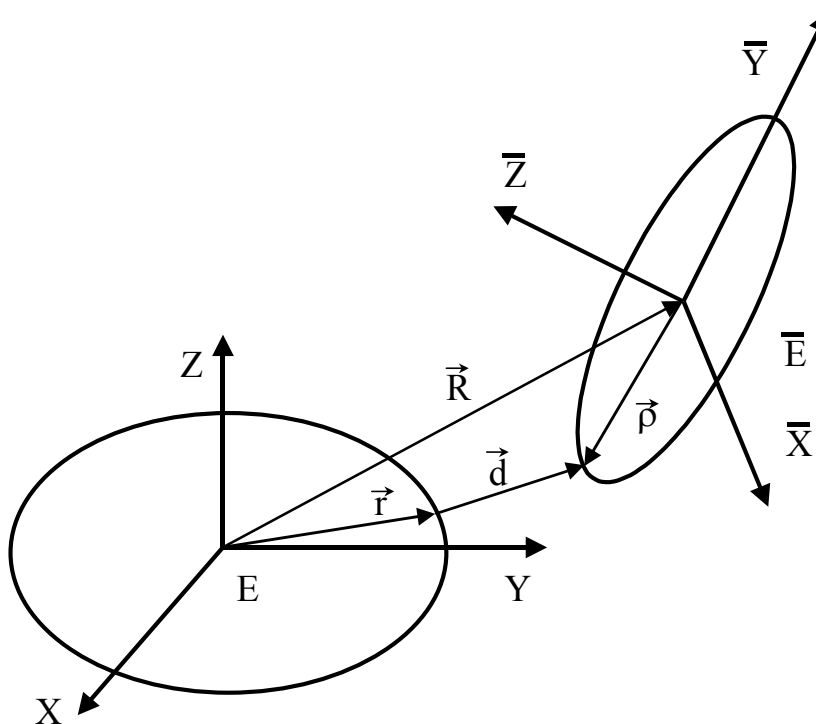

Figure 1. Two ellipsoids of arbitrary shape and orientation

The minimum distance is found by minimizing the square distance between points that are constrained to lie on the ellipsoids. Let $\vec{r} = (x, y, z)^T$ be a point on E expressed in E; let $\vec{\rho} = (\overline{x}, \overline{y}, \overline{z})^T$ be a point on $\overline{E}$ expressed in $\overline{E}$. The constraint equations become

$$\phi(x, y, z) = \vec{r}^T D \vec{r} - 1 = 0,\qquad(1)$$
$$\overline{\phi}(\overline{x}, \overline{y}, \overline{z}) = \vec{\rho}^T \overline{D} \vec{\rho} - 1 = 0,\qquad(2)$$

where

$$D = \begin{bmatrix} \dfrac{1}{a^2} & 0 & 0 \\ 0 & \dfrac{1}{b^2} & 0 \\ 0 & 0 & \dfrac{1}{c^2} \end{bmatrix} \text{ and } \overline{D} = \begin{bmatrix} \dfrac{1}{\overline{a}^2} & 0 & 0 \\ 0 & \dfrac{1}{\overline{b}^2} & 0 \\ 0 & 0 & \dfrac{1}{\overline{c}^2} \end{bmatrix}.\qquad(3)$$

The relative distance vector between the points, expressed in E, is $\vec{d} = \vec{R} + M\vec{\rho} - \vec{r}$ and the square distance is $d^2 = \vec{d}^T\vec{d}$. Introducing Lagrange multipliers λ and $\overline{\lambda}$, the augmented objective function is

$$F(x,y,z,\lambda,\overline{x},\overline{y},\overline{z},\overline{\lambda}) = d^2 + \lambda\phi + \overline{\lambda}\,\overline{\phi} \tag{4}$$

Points on the two ellipsoids for which the relative distance is minimum are found by setting the derivative of F with respect to each of its arguments to zero. The derivatives with respect to the multipliers simply recover Eqs. (1) and (2). The additional equations are

$$\vec{r} - \vec{R} - M\vec{\rho} + \lambda D\vec{r} = 0, \tag{5}$$

$$-M^T\vec{r} + M^T\vec{R} + \vec{\rho} + \overline{\lambda}\,\overline{D}\vec{\rho} = 0 \tag{6}$$

Eqs. (1), (2), (5), and (6) are 8 coupled quadratic equations for the 8 unknowns that must be solved to determine the minimum distance.

While the formulation of the equations is rather straight-forward, determining solutions to these equations can be quite difficult for several reasons. First, there are multiple solutions to the equations because the equations describe conditions for both the maximum and minimum relative distance. Second, there may be multiple values for $\vec{r}$ or $\vec{\rho}$ that generate the same distance, i.e., there is an unknown number of solutions to the equations. Lastly, a numerical nonlinear equations solver such as Newton-Raphson must be used to find solutions, and such methods typically only converge to a solution given a sufficiently good guess. These difficulties led us to pursue an alternate strategy.

Consider the problem of determining the closest distance from a point $\overline{P}$ to ellipsoid E. Let $\vec{R}$ locate $\overline{P}$ expressed in E. The minimum distance problem can be generated from the above formulation by setting $\vec{\rho} = 0$ and $\overline{\lambda} = 0$. This results in Eq. (1) and in a modified Eq.(5)

$$\vec{r} - \vec{R} + \lambda D\vec{r} = 0. \tag{7}$$

Solving, we find

$$\vec{r} = (I + \lambda D)^{-1}\vec{R} \tag{8}$$

where I is the identity matrix. Substituting into Eq. (1), we find 1 equation for the 1 unknown λ

$$\vec{R}^T(I + \lambda D)^{-T}D(I + \lambda D)^{-1}\vec{R} - 1 = 0. \tag{9}$$

An equivalent result was derived using only geometrical arguments in a paper by Tang[9]. Eq. (9) can be solved using many methods, e.g., Newton iteration. Of course, there are multiple solutions to Eq. (9) representing the minimum and maximum distance cases between $\overline{P}$ and E.

It is very instructive to look for the geometrical meaning of the solutions to Eq. (9). Noting that $\vec{\rho} = 0$, Eq. (7) can be solved for $\vec{d}$ to yield

$$\vec{d} = \lambda D\vec{r}. \tag{10}$$

The vector $D\vec{r}$ is an outward normal vector to the ellipsoid surface at $\vec{r}$. Thus, the shortest relative distance vector from the surface to $\bar{P}$ lies normal to the surface. In fact, Eqs. (5) and (6) indicate that the shortest relative distance vector between ellipsoid surfaces is normal to both ellipsoids. Multiplying by $\vec{r}^T$ and using Eq. (1), we also see that

$$\lambda = \vec{r}^T \vec{d}, \tag{11}$$

so that the sign of λ can be inferred from the geometry of the solution.

We now make use of the convexity of the ellipsoid surface. If $\bar{P}$ lies outside the surface of E, then the shortest $\vec{d}$ necessarily points outward from the surface at $\vec{r}$, so that $\lambda > 0$. Moreover, the minimum distance and the closest point $\vec{r}$ on the ellipsoid are unique, implying that there is only 1 solution to Eq. (9) with positive λ for any point $\bar{P}$ outside of E. For $\bar{P}$ outside of E, the existence and uniqueness of the solution to Eq. (9) is no longer in doubt and any competent numerical scheme will be able to determine the solution. For $\bar{P}$ inside of E, however, an unknown number of solutions exists.

STRATEGY

Rather than solving the eight nonlinear simultaneous equations for determining the closest distance between ellipsoids, we begin by first solving for the closest distance between a point $\bar{P}$ on $\bar{E}$ to the surface of ellipsoid E. The solution identifies the closest point P on E (given by the vector $\vec{r}$). We then solve the problem of determining the closest distance from P on E to the surface of ellipsoid $\bar{E}$. This problem will identify a new point on $\bar{E}$ to be used as $\bar{P}$. The iteration scheme continues until the distance between the ellipsoids (i.e., between $\bar{P}$ and P) no longer changes significantly. At that point, one may choose to solve the simultaneous equations directly using $\bar{P}$ and P as initial guesses. This iteration scheme is illustrated in Figure 2.
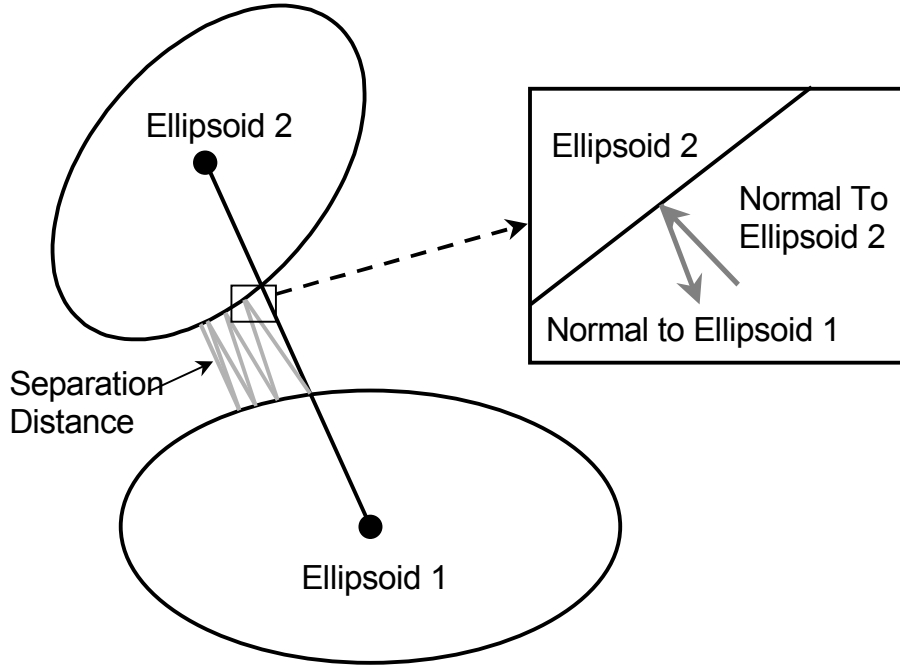
Figure 2. Iteration scheme for computing ellipsoid separation

To speed the solution of Eq. (9) that is required during each iteration, a seed value of λ from the previous computation is used as the initial guess. After a few iterations between ellipsoids, the seed value of λ used for Eq. (9) is such a good initial guess that Eq. (9) itself is solved without performing many iterations.

Convergence. Because the iterative scheme chooses candidate points along the surface normals, the scheme converges faster the further the ellipsoid surfaces are apart. As the surfaces become closer together, more iterations are required because the candidate points move slowly along the surfaces whenever the normals are nearly aligned. Setting a maximum number of allowed iterations prevents the routine from performing an infinite loop.

Intersection. While iterating, each point is tested for whether or not it lies inside the ellipsoid surface, thereby determining whether the ellipsoids have intersected. For example, if

$$\vec{r}^{T} D \vec{r} < 1 \tag{12}$$

then $\overline{P}$ lies inside E. When the ellipsoids have intersected, a new definition of distance between ellipsoids is required if a measure of the degree of intersection is desired.

In some cases, the iterative scheme cannot distinguish tangency from intersection. Consider the condition shown in Figure 3 where the iterative scheme converges toward a point of intersection from the outside. In such a case, the scheme fails to detect intersection.
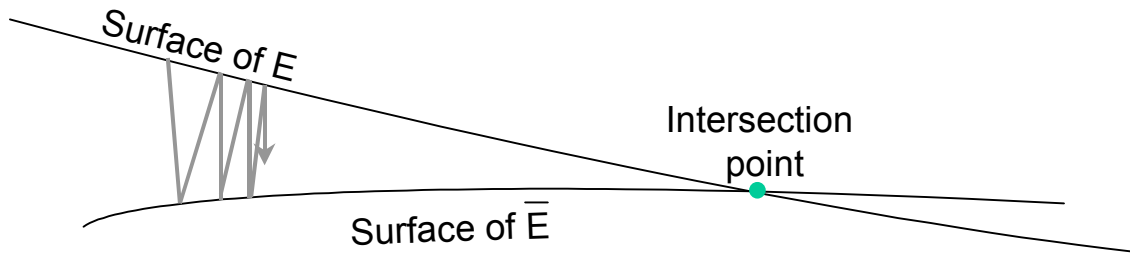
Figure 3. This sequence converges toward the intersection point and does not detect that the ellipsoids have intersected.

To account for these problems, the solution found from the iterative scheme is tested in two ways. First, if the distance is very small, nearby points are checked to determine whether intersection has occurred. Second, a check is performed to determine if the computed $\vec{d}$ indeed is normal to the surface at $\vec{r}$. If not, a grid search is used to determine the closest points on each surface. The search begins by creating on each ellipsoid an equally-spaced ring of points lying on the surface of the ellipsoid centered on the current best solution. The distances between points on each ring is then computed to test whether any pair of points are closer than the current best solution. If a closer pair is found, then new rings are created using this pair and the procedure continues. Every time a new pair of closest points is found, the tests for intersection are performed. If no closer pair is found, then smaller rings are used. The routine stops whenever the distance changes insignificantly or intersection is detected.

Filters. The computational cost of determining the distance between two arbitrary ellipsoids increases the importance of the use of filters. While the most commonly used tests were originally designed for the case where only a minimum allowed separation distance was specified, they are easily adapted to the current problem. The simplest adaptation of the filters is to sum the maximum dimension of the threat volume for the primary satellite with that of each secondary object to yield a separation distance which can be used in a minimum separation distance analysis. Only the set of secondary objects which are not rejected on the basis of minimum separation distance are subjected to the ellipsoidal threat volume analysis.

EXAMPLE

Example threat analyses were performed using an IRIDIUM™ satellite, SSC number 24836, as the primary object and a set of 7819 secondary objects from the Space Surveillance Catalog over a four day interval. In the first analysis, the threat volumes associated with the primary and secondary objects were defined as spheres with constant radii. In the second analysis, the threat volumes associated with the primary and secondary objects were defined as ellipsoids with constant dimensions. The dimensions of the ellipsoids and spheres are shown in Table 1. A minimum separation distance between threat volumes of one kilometer was used in both cases.

Table 1. DIMENSIONS OF THREAT VOLUMES IN KM

OBJECT	TANGENTIAL	CROSS-TRACK	NORMAL	SPHERICAL RADIUS
Primary	1.0	0.5	0.5	1.0
Secondary	4.0	2.0	1.0	4.0

Fourteen instances of close approaches were detected when spherical threat volumes were considered over the analysis window, while only eight were detected using the ellipsoidal threat volumes. The detected close approach periods for the spherical case and the ellipsoidal case are shown in Table 2 and Table 3 respectively. The lower number of close approaches detected using ellipsoidal threat volumes is due to the relative geometry during the interval around the time of closest approach. The decrease in the number of reported close approaches is smaller than usual for this case due to repeating geometry between the primary satellite and SSC 25274. Figure 4 shows the relationship between the primary and secondary threat volumes for the case where the IRIDIUM™ satellite has a close approach using spherical threat volumes with SSC 24197. Figure 5 shows the same relationship when the ellipsoidal threat volumes are used. Because the separation distance between the ellipsoids remained greater than one kilometer, no close approach event occurred.

Table 2. CLOSE APPROACHES USING SPHERICAL THREAT VOLUMES

SSC #	DURATION (SEC)	MIN RANGE (KM)
20898	0.111	5.942
22327	0.022	5.998
18997	0.437	5.091
24197	1.008	3.964
13649	0.702	3.183
13649	0.419	5.173
25274	0.496	5.682
25274	1.369	2.763
25274	1.541	0.251
25274	1.321	3.095
25274	1.150	3.988
25274	1.501	1.324
25274	1.431	2.210
25274	0.838	5.032

Table 3. CLOSE APPROACHES USING ELLIPSOIDAL THREAT VOLUMES

SSC #	DURATION (SEC)	MIN SEPARATION (KM)	MIN RANGE (KM)
13649	0.375	0.598	3.183
25274	0.908	Intersect	2.763
25274	1.069	Intersect	0.251
25274	0.863	Intersect	3.095
25274	0.638	0.137	3.988
25274	0.983	Intersect	1.324
25274	0.915	Intersect	2.210
25274	0.264	0.833	5.032

CONCLUSIONS

We have presented a method for determining close approach events for objects having ellipsoidal threat volumes. Ellipsoid shapes provide a method for distinguishing different levels of position uncertainty in three orthogonal directions, providing more realistic model than a simple worst-case approach. By defining conjunctions as those times at which the minimum separation distance between ellipsoids is less than a user-specified threshold, the number of close approach events is reduced when compared to analyses based only on range. This is believed to be a reasonable technique for reporting close approaches when realistic covariance information for all objects is not available.
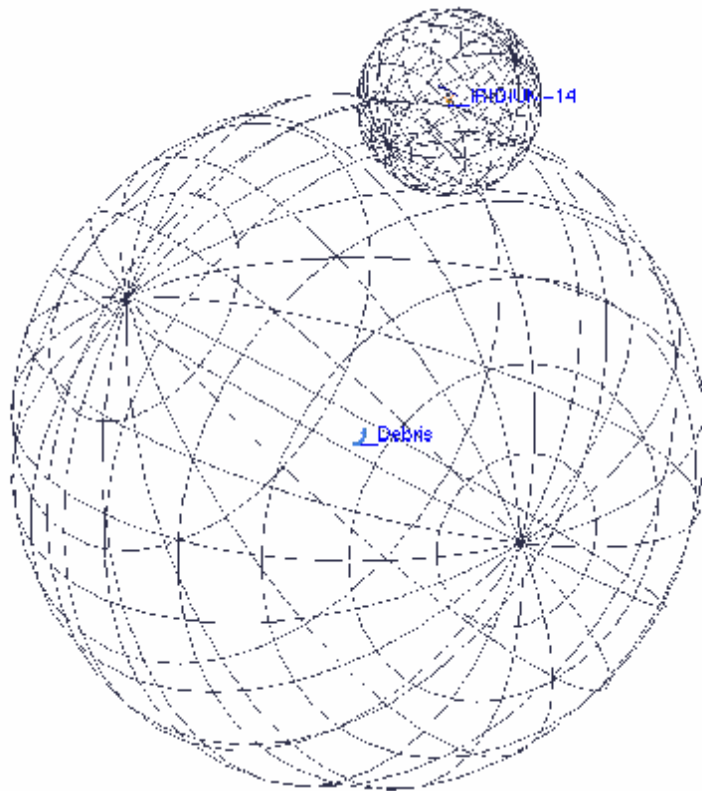
Figure 4. IRIDIUM™ satellite and debris near TCA with spherical threat volumes
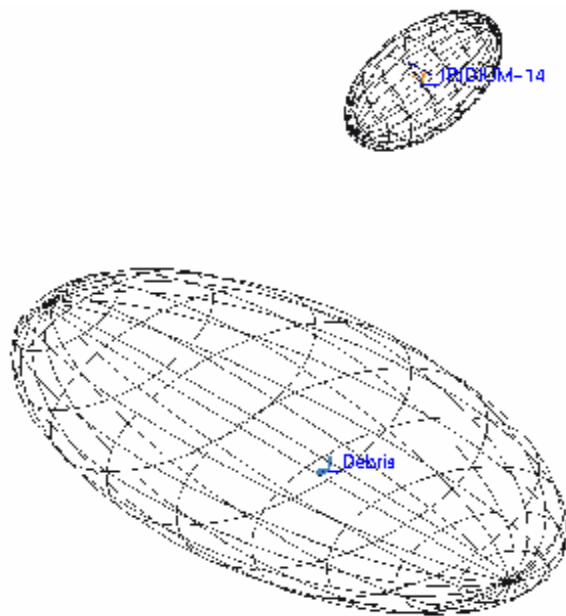

Figure 5. IRIDIUM™ satellite and debris near TCA with ellipsoidal threat volumes

REFERENCES

[1] JENKINS, E.L. and SCHUMACHER, P.W. "Predicting Conjunctions with Trackable Space Debris: Some Recent Experiences", Paper No. 97-014, 20th Annual AAS Guidance and Control Conference, Breckenridge, Colorado, February 5-9, 1997.

[2] ALFRIEND, K.T., AKELLA, M.R., LEE, D., WILKINS, M., FRISBEE, J. and FOSTER, J.L. "Probability of Collision Error Analysis", Paper No. AIAA-98-4279, AIAA/AAS Astrodynamics Specialists Conference, Boston, MA, August 1998.

[3] HOOTS, F.R., CRAWFORD, L.L. and ROEHRICH, R.L. "An Analytic Method to Determine Future Close Approaches Between Satellites", *Celestial Mechanics*, Vol. 33, 1984, pp. 143-158.

[4] WOODBURN, J. and DICHMANN, D. "Determination of Close Approaches for Constellations of Satellites", Paper No. C-5, IAF International Workshop on Mission Design and Implementation of Satellite Constellations, Toulouse, France, November 1997.

[5] DYBCZNSKI, P.A., JOPEK, T.J. and SERAFIN, R.A. "On the Minimum Distance Between Two Keplerian Orbits with a Common Focus", *Celestial Mechanics*, Vol. 38, 1986, pp. 345-356.

[6] BEERER, J. and BAUER, T. "Determination of Closest Approach and Duration of Encounter for Two Satellites in Circular Non-Coplanar Orbits", Paper No. 83-336, AAS/AIAA Astrodynamics Conference, Lake Placid, New York, August 1983.

[7] ALFANO, S. and NEGRON, D., JR. "Determining Satellite Close Approaches", *The Journal of the Astronautical Sciences*, Vol. 41, No. 2, April-June 1993, pp. 217-225.

[8] ALFANO, S. "Determining Satellite Close Approaches, Part II", *The Journal of the Astronautical Sciences*, Vol. 42, No. 2, April-June 1994, pp. 143-152.

[9] TANG, C. "Geodetic Altitude to a Triaxial Ellipsoidal Planet", *The Journal of the Astronautical Sciences*, Vol. 36, No. 3, July-September 1988, pp. 279-283.